Electrical Power and Energy Systems 115 (2020) 105489

Contents lists available at ScienceDirect

Electrical Power and Energy Systems

journal homepage: www.elsevier.com/locate/ijepes

Measuring method for partial discharges in a high voltage cable system subjected to impulse and superimposed voltage under laboratory conditions

Jiayang Wu*, Armando Rodrigo Mor, Paul V.M. van Nes, Johan J. Smit

Delft University of Technology, Electrical Sustainable Energy Department, Mekelweg 4, 2628CD Delft, the Netherlands

ARTICLE INFO

Keywords:
Partial discharge measuring method
High voltage cable joint
Superimposed voltage conditions
High frequency current transformer
Band-pass filter

ABSTRACT

A partial discharge (PD) measuring system has been deployed in order to identify and measure PD in a high voltage (HV) cable joint under impulse and superimposed voltages under laboratory conditions. The challenge is to enable the detection of PD during the impulse conditions. The method of measurement has been investigated by introducing an artificial defect in the cable joint in a controlled way to create conditions for partial discharges to occur. Next the HV cable system is subjected to AC, impulse and superimposed voltage. Two high frequency current transformers (HFCT) installed at both ends of the cable joint were used to identify PD from the cable joint and to separate PD from disturbance. Transient voltage suppressors and spark gaps are applied to protect the measuring equipment. Band pass filters with selected characteristics are applied to suppress transient disturbances and increase the chance to detect PD during the impulse. PD signals are separated from transient disturbances during data post processing and by means of pulse polarity analysis. The developed system enables the detection of so-called main and reverse discharges respectively occurring during the rise and tail time of the superimposed impulse. The measurement results obtained show the effectiveness of the presented PD measuring system for investigating the effects of voltage transients on a HV cable system in laboratory conditions.

1. Introduction

Partial discharge measurements provide a useful tool to obtain information about discharging defects in high-voltage equipment. In power cables, PD occurs at insulation defects in particular in cable joints and terminations, especially at interfaces [1]. Therefore, PD measurement on cable systems can be considered a useful tool to diagnose insulation condition for both laboratory application and on-site application [2–4].

PD in power cables is normally measured under AC voltage by using the conventional technique defined by IEC 60270 [5]. In practice, power cables are not only subjected to AC operating voltage, but also to transient voltages such as lightning and switching impulses, which occasionally will be superimposed on the normal AC voltage. Those transient voltages will have an additional stress on the cable insulation. In that regard it is important to investigate PD under impulse and superimposed voltages.

One of the challenges in measuring PD under impulse and superimposed voltages concerns the suppression of the disturbances caused by the transient voltages. In laboratory tests, the applied impulse voltage causes currents in the cable under test that disturb the PD measurement. So the PD measurement system needs to have a strong suppression of the disturbance. In such a case, the conventional PD technique is not suitable anymore. The unconventional method based on the measurements of electrical signals in MHz range is of more interest as a better alternative for these conditions [4,6–10].

Three circuits for PD detection under impulse are provided in [11] with a measurement frequency from hundreds of MHz to GHz, namely: the high frequency current transformer (HFCT) with multipole filter, the coupling capacitor with multipole filter, and the electromagnetic couplers. HFCTs or other sensors are commonly used with wide/ultra-wide bandwidth together with filters and a digital oscilloscope to detect PD in insulation specimens or models under impulses [12–17]. A coupling capacitor was used to measure PD in material samples in cases where only impulse [18] and square wave voltage were applied [5]. Those PD measuring systems were able to detect PD during the impulse even during its front time. For superimposed impulses, PD was detected in laminated paper using a current transformer and a high-pass filter by Hayakawa et al. [19]. Nikjoo et al. [20] used a wideband detection system consisting of a coupling capacitor, a detection impedance and a low-pass filter to measure PD in oil-impregnated paper. However, in both works, PD was measured during AC cycles before and after impulses instead of during the impulses. Moreover, PD measurements in the above-mentioned works were performed on material specimens.

* Corresponding author.
E-mail address: j.wu-3@tudelft.nl (J. Wu).

https://doi.org/10.1016/j.ijepes.2019.105489
Received 13 May 2019; Received in revised form 14 June 2019; Accepted 15 August 2019

Due to the small scale of the samples and the relatively low voltage level, less disturbance is produced in the circuitry.

Regarding PD measurement on power cables, for off-line tests capacitors and HFCTs are normally used, while on-line tests almost always use HFCTs [2], especially for testing cable accessories [21–23]. However in related literature, partial discharges in power cables are usually measured after the impulse has been applied, while partial discharges during the moment of impulse have been less reported.

During impulse voltage conditions the PD measuring system should fulfil two requirements. Firstly, the safety of both human and equipment need to be ensured when using the measuring system. Secondly, the measuring system should be able to detect PD from the cable joint before, during and after the impulse transient application upon the AC voltage.

This work presents a PD measuring system for laboratory use which is able to measure PD during impulses in a HV cable system under impulse and superimposed voltages. A 150 kV cross-linked polyethylene (XLPE) cable system with an artificial defect in the cable joint was tested under lab conditions. A PD measuring system consisting of two HFCTs, band-pass filters, transient voltage suppressors (TVS Diode Array WE-TVS) and a digital oscilloscope was used.

In particular, the two HFCTs were installed at both ends of the cable joint, which helped to identify the PD from the cable joint and separate PD from disturbance signals using the polarity of the pulses. TVSs were added after the filters for protection purpose.

This measuring system is able to identify and measure PD in AC and during the superimposed transients. Since the impulses applied to the cable system were in the range of hundreds of kilovolt, very large disturbances were induced during the impulse application, due to which PD cannot be detected during the impulse front time without additional filtering. To decrease the latter disturbance of the PD signals, additional band-pass filters were added. The possibility of the PD measuring system to measure PD during impulses is of potential use for studying the effects of transients on HV cable and accessories.

The following chapters describe in detail the test setup and the characteristics and particularities of the proposed measuring system for PD cable measurements under transients.

2. Set-up description

The circuit consists of the HV cable system under test, the testing voltage supplies and the PD measuring system. Fig. 1 shows the schematic diagram of the test circuit. Values of all the elements are given except for the resistors in the impulse generator, which are adjusted according to the required waveforms of impulse voltages. For testing under impulse voltages, part of the circuit denoted by the grey area in Fig. 1 was connected. For testing under superimposed voltages, the entire circuit was connected. Fig. 2 shows the physical set-up as built in the HV lab based on Fig. 1. In this work, a 150 kV XLPE extruded cable system was used as test object. The HV cable system was tested under 50 Hz AC voltage, impulse voltage and superimposed voltage. To identify and measure PD in the HV cable system, an unconventional PD measuring system was installed at the cable joint. A conventional PD measuring system according to standard IEC 60270 was also used. Detailed explanations on the setup are given in the following chapters.

2.1. HV cable system

The test object is a 16-m long 150 kV cable terminated with two outdoor-type terminations, termination 1 and 2, and a pre-moulded joint in between, as shown in Fig. 2. The joint is located five meters from the termination 2. The cable is grounded at both cable terminations. The capacitance of the cable system is 3.75 nF.

In order to investigate the functionality of the PD measuring system in the laboratory condition, a PD source is needed to produce PD in the cable joint. In this work, an artificial defect was created by manipulating the joint. The connector in the joint was prepared in such a way that the cable can be pulled out of the joint. In practice, this will not happen in a properly mounted cable joint. Whereas for laboratory testing, this defect can produce stable partial discharges. In this work, the cable was pulled 7 mm out of the joint at the side near to termination 2. For research purposes, this set up can generate under AC voltage detectable PD activities with recognizable and stable phase-resolved PD patterns (PRPD). On average, the partial discharge inception voltage (PDIV) of the partial discharge was 104 kV_{rms}. Fig. 3 shows the way in which the artificial defect is created by pulling out of the HV cable joint.

2.2. Generation of impulse and superimposed transient voltages

The test circuit is able to provide 50 Hz AC voltage, impulse voltage and superimposed voltage. To supply AC voltage, a 380 V/150 kV AC transformer was connected to the HV cable. A LC low-pass filter (L_1, L_2, C_1, C_2) was added at the low-voltage side of the transformer to filter out the line noise. Five stages of a Marx generator were used to provide impulse voltages. The total discharge capacitance C of the five stages is 100 nF. Different impulse waveforms, i.e. different front time T_f and time to half value T_h, can be generated by adjusting the front resistor R_f and the tail resistors R_{h_LI} and R_{h_SI}. At the same time, T_f and T_h are also related to the total load capacitance C_{load}. For testing under superimposed voltages, the total load capacitance C_{load} is the combination of the HV cable, the voltage divider VD_2, the blocking capacitor C_b, the coupling capacitor C_k and the filtering capacitor C_d. In order to reach a longer front time without using a too large R_f, an additional 1 nF capacitance C_l was connected [24]. The settings of the impulse generator for generating different impulses in this work are given in Table 4 in the

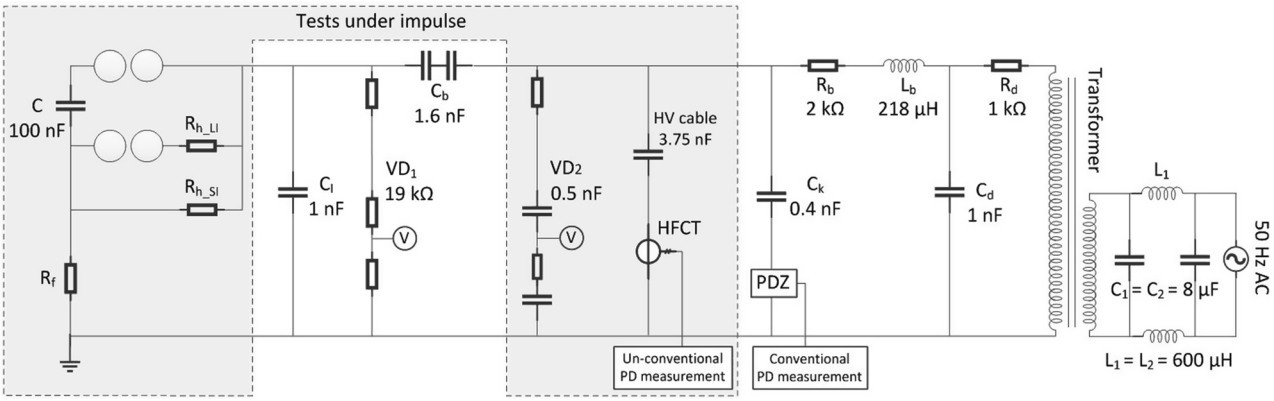

Fig. 1. Test circuit.

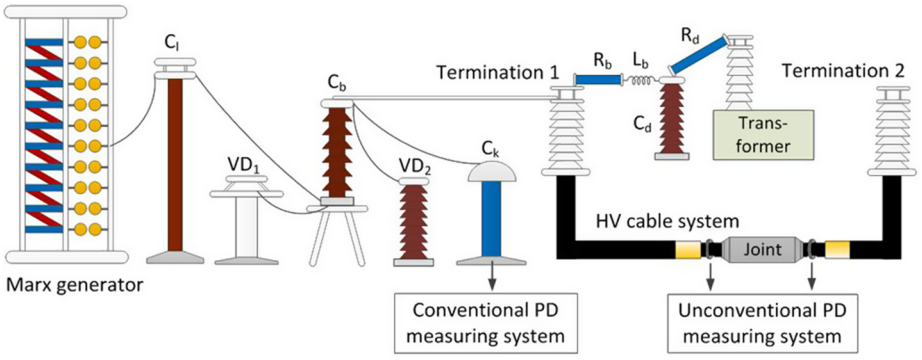

Fig. 2. Physical set-up.

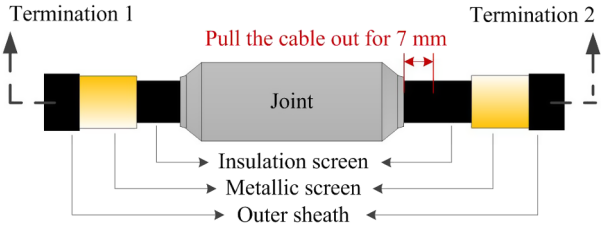

Fig. 3. HV cable joint and the artificial defect.

Appendix.

For generating superimposed voltages, the AC transformer and the impulse generator were both connected to the cable. In order not to stress the impulse generator with the AC voltage, a 1.6 nF blocking capacitor C_b together with a 2 kΩ resistor R_b were installed between the AC supply and the impulse supply. This attenuates the AC voltage at the impulse generator and allows the impulse voltage to be superimposed on AC voltage at the cable. The AC transformer was protected against the impulse voltages by a RC low-pass filter (R_d, C_d). One voltage divider VD_1 was used to measure the generated impulse voltages at the impulse generator, and another VD_2 served to measure the composite voltages at the cable termination 1.

In this work, the HV cable system was tested under AC voltage, impulse voltage and superimposed voltage. Fig. 4a shows the waveform of the impulse voltage having a peak value V_{peak}, front time T_f and time to half value T_h. The waveform of the superimposed voltage is shown in Fig. 4b. An impulse voltage with front time T_f and time to half value T_h is riding on the AC wave crest. The total peak value V_{peak} of the testing voltage is the combined value of the AC peak value V_{ACpeak} and the superimposed impulse voltage.

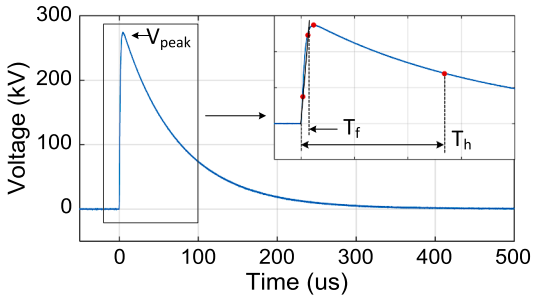

(a). Test voltage waveform of impulse voltage.

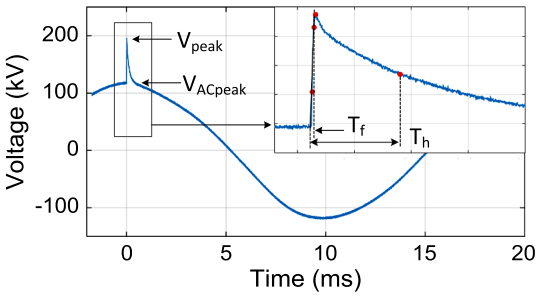

(b). Test voltage waveform of superimposed voltage.

Fig. 4. Test voltage waveforms.

2.3. PD measuring system

Two identical HFCTs were used to detect PD from the cable joint. The two HFCTs have a gain of 3 mV/mA and a bandwidth of 100 kHz–40 MHz [25]. The PD signals captured by the two HFCTs were transmitted through two 20-m identical coaxial cables to a digital oscilloscope Tektronix MSO58, which was used to acquire the signals with

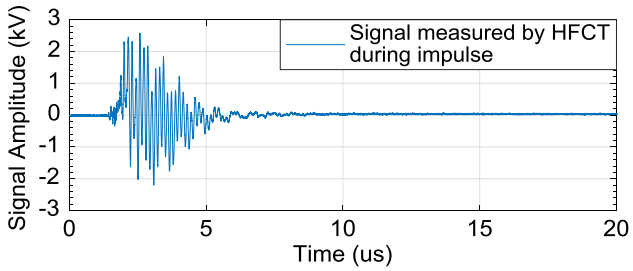

Fig. 5. Signal measured by HFCT during the impulse application.

a sampling frequency of 1.25 GS/s and a bandwidth of 250 MHz.

During the application of impulse voltages, transient currents in the cable induce a high voltage signal in the HFCTs. Fig. 5 presents the signal measured by the HFCT during the application of the impulse. The signal was measured with a HV probe. The impulse has a waveform as shown in Fig. 4a with V_{peak} of 274 kV and T_f/T_h = 3/2000 µs, which was one of the test voltages applied on the cable in the PD measurement. As shown in Fig. 5, the amplitude of the measured signal is in the range of kilovolt, which far exceeds the maximum input voltage of the oscilloscope. Such large signal will cause a damage to the oscilloscope. Therefore, in order to protect the oscilloscope, a filter/suppressor protection unit was applied before the oscilloscope. A transient voltage suppressor (TVS) together with a spark gap were used to clip the voltage to 12 V. A band-pass filter with bandwidth of 114 kHz–48 MHz was added before the TVS to reinforce the power attenuation outside the sensor's bandwidth. The TVS, the spark gap and the band-pass filter are integrated in one box, named filter A. Fig. 6a shows the configuration of the measuring system combined with the HFCT, the coaxial cable, and the integrated unit filter A. The transfer functions of the HFCT as well as the measuring system are characterized by using the method in [26] and given in Fig. 6b.

The two HFCTs were mounted at both ends of the joint with the same polarity, as shown in Fig. 7. The one near to termination 1 is named as HFCT 1, and the other one near to termination 2 is named as HFCT 2. When the PD occurs externally to the cable joint, i.e. from the cable section near termination 1 or termination 2, the PD signals measured by HFCT 1 and HFCT 2 from PD event have the same polarities and similar magnitudes. If the PD occurs in the cable joint, the PD

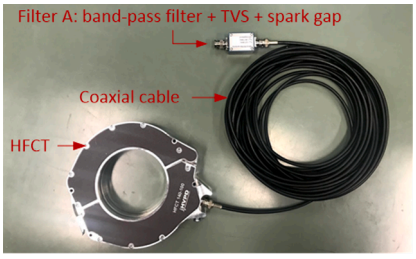

(a). Configuration of measuring system combined with HFCT, filter A and the connecting coaxial cable.

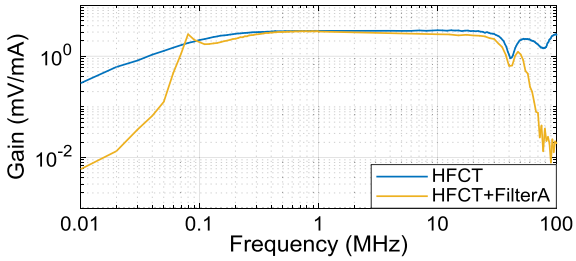

(b). Characteristics of HFCT and the measuring system combined with HFCT, filter A and the connecting coaxial cable.

Fig. 6. Configuration and characteristics of the measuring system.

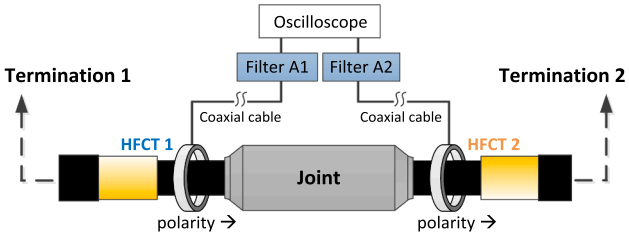

Fig. 7. Two HFCTs installed at two ends of cable joint.

is generated between the two HFCTs and splits propagating in both directions. In this case the PD pulses measured by HFCT 1 and HFCT 2 have opposite polarities and similar magnitudes. By using this polarity recognition, it is possible to discriminate between discharges produced in the joint and outside the joint.

PDflex [27], software developed by the High Voltage Laboratory of Delft University of Technology, was used for analyzing and presenting the PD measurement results with phase-resolved PD patterns (PRPD), time-resolved PD pulses (TRPD) and typical PD parameters [28,29]. A clustering technique applied in PDflex helped to separate PD from noise.

3. Verification of the PD measuring system

To verify the functionality of the PD measuring system, three types of pulses were injected in the cable system from different locations. Table 1 lists the verifying pulses and the testing voltages under which they were tested. The following chapters describe the results for each case.

3.1. Injected pulses

For verification, pulses of 1 nC were injected into the measuring system from different locations both internally and externally to the cable joint. Fig. 8 illustrates how to simulate pulses occurring in the cable joint with the calibrator. The results recorded by HFCT 1 and HFCT 2 are shown in Fig. 9.

When the calibration pulses were from termination 1, the measured signals always have positive polarities and similar amplitudes, as shown in Fig. 9a. When the calibration pulses were from termination 2, the measured signals show negative polarities, as shown in Fig. 9b. In Fig. 9c when the calibration pulses were from the cable joint, the pulse captured by HFCT 1 shows a negative polarity while the pulse captured by HFCT 2 shows a positive polarity.

It can be seen from the above results that, the applied PD measuring system is able to indicate whether the pulses are internal or external to the cable joint by polarity recognition. If there are PD occurring in the joint while disturbances are produced outside the joint, such polarity recognition can also help to separate PD from disturbances.

3.2. Corona discharges

To test real PD external to the cable joint, corona discharge was generated by a metal needle installed at termination 1 under an AC voltage of 16 kV_{rms}. Fig. 10 shows the PRPD patterns of the corona

Table 1
Verifying pulses and their testing voltages.

PD sources	Locations	Testing voltages
Injected pulse (1 nC from calibrator)	Ternimation1 Termination 2 Cable joint	No voltage applied
Corona discharge	Termination 1	AC = 16 kV_{rms}
Surface discharge	Cable joint	AC = 108 kV_{rms}

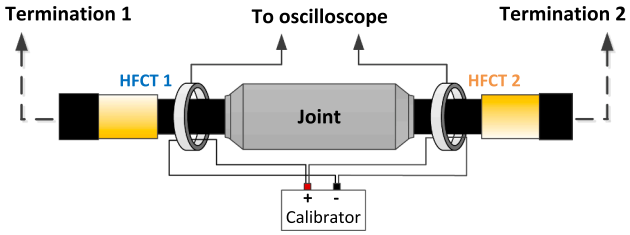

Fig. 8. Pulses simulated from the cable joint.

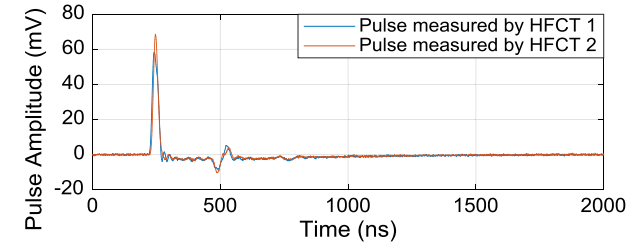

(a). Pulse injected from termination 1.

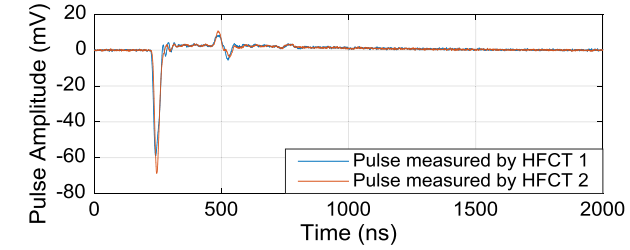

(b). Pulse injected from termination 2.

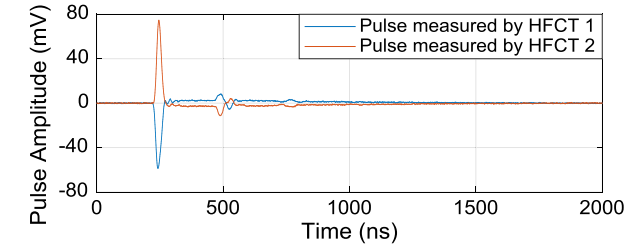

(c). Pulse simulated from the cable joint between two HFCTs.

Fig. 9. Injected pulses measured by HFCTs.

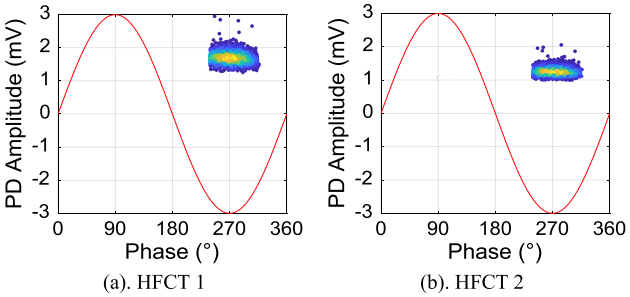

(a). HFCT 1 (b). HFCT 2

Fig. 10. PRPD patterns of corona discharges at termination 1.

measured by HFCT 1 and HFCT 2. Both patterns indicate that the positive corona discharges occurred at the peak of negative AC cycle. Fig. 11 shows the TRPD pulses of one corona discharge measured by the two HFCTs. Both PD pulses have positive polarities, which is in accordance with the case of Fig. 9a, where the pulse was injected from termination 1. So based on the polarities of the corona pulses, it can be confirmed that the corona source is external to the cable joint and from the cable section near to termination 1.

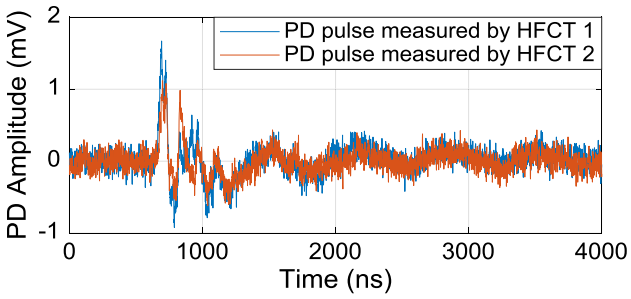

Fig. 11. TRPD pulses of one corona discharge at termination 1.

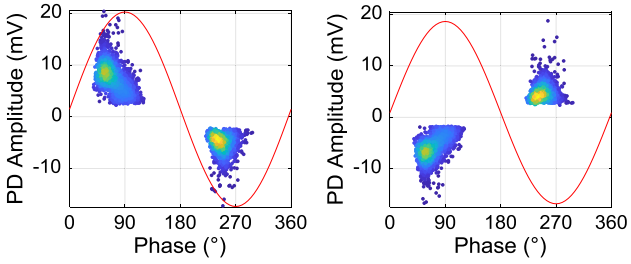

(a). HFCT 1 (b). HFCT 2

Fig. 12. PRPD patterns of partial discharges at 108 kV_{rms}.

3.3. Partial discharges

The partial discharges generated by the artificial defect in the cable joint were measured at an AC voltage of 108 kV_{rms}. Fig. 12 shows the PRPD patterns of the partial discharges measured by HFCT 1 and HFCT 2. With HFCT 1, PDs measured under positive half cycle possess positive polarities and negative polarities under negative half cycle. With HFCT 2 the PD polarities reverse. So the pulses measured by the two HFCTs from every discharge event always have opposite polarities, which confirms that the PDs originate from the cable joint internally.

Fig. 13 shows the TRPD pulses of measured partial discharges. One partial discharge event occurred during the negative half cycle is shown in Fig. 13a. The first peaks of the two pulses have opposite polarities: the pulse measured by HFCT 1 has negative polarity while the pulse

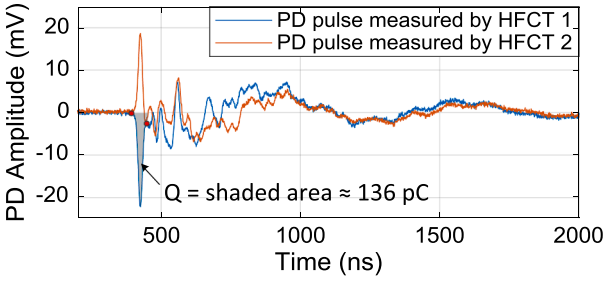

(a). TRPD pulses of one partial discharge at negative cycle of 108 kV_{rms}.

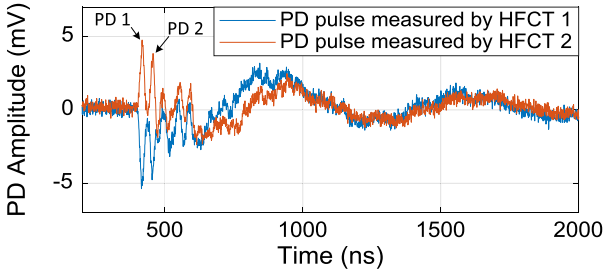

(b). TRPD pulses of two partial discharges in series at 108 kV_{rms}.

Fig. 13. TRPD pulses of partial discharges measured by HFCTs.

measured by HFCT 2 has positive polarity. These two pulses all reach the peak values at the same time. After the first peak, both pulses start to attenuate quickly with oscillation due to the circuit configuration and cable reflections. Based on the pulse characteristics, only the first peak of each pulse was used to analyse the PD information. Due to the polarity, these two pulses indicate that the partial discharge source is located in the cable joint. Since the duration of the first peak is in the range of 40–50 ns, two PDs within a time interval longer than 40 ns should be detectable. Fig. 13b shows a case in which two PD events occurred in series with a time interval of 40 ns.

It is worth mentioning that since the magnitude of the partial discharges is in the order of millivolt, the partial discharges would not be clipped by the TVS.

Fig. 13a also gives an estimation of the charge magnitude of the PD pulse measured by HFCT 1. The apparent charge Q, with estimated value of 136 pC, is calculated as the integral of the first peak over time by applying the method in [27,28]. Such estimation is valid when the PD pulse is not critically affected. However, since the cable length under test is quite short, the impact on PD pulse shape increases a lot due to pulse propagation and reflections. This situation will be shown in later sections. In such case, the estimation of apparent charge is not accurate any more. Consequently, the calibration of PD value based on the measured PD pulse becomes difficult. Thus, we directly use the voltage amplitude of the first PD pulse to describe the PD level instead of the charge magnitude.

3.4. PD measured with conventional method

As stated in [8], depending on the test object and the PD measuring system there is no obvious correlation between the apparent charge level measured with the conventional and the unconventional methods. Moreover, in short cables the PD measurements are affected by the multiple PD reflections which makes the calibration process difficult. However, to provide some reference information, a conventional PD measuring system was also applied in the test circuit to measure PD under the same AC condition. A 400 pF coupling capacitance C_k was connected to the cable termination 1. A Haefely DDX9101 PD detector complying with IEC 60270 [5] was used to measure PD through a PD coupling impedance PDZ. The PD measurement result acquired by the conventional method is given in Fig. 14. For the same defect and the same AC condition of 108 kV_{rms} as in Section 3.3, Fig. 14 shows a comparable PRPD pattern to Fig. 12. The average discharge magnitude of 514 pC, which was measured with a filter bandwidth of 50–400 kHz, is in the same order of magnitude as the estimated charge value as shown in Fig. 13a. In addition, the conventional PD calibrator also helped to check the sensitivity of the PD measurement. The sensitivity around 10 pC was reached by diminishing calibration pulses injected into the cable system until it cannot be observed.

4. PD measurements

To evaluate the intended capability of the PD measuring system, the cable system was then tested under impulse voltages and superimposed voltages. Table 2 lists the tests and the testing voltages with their parameters, as defined in Fig. 4. The following chapters describe the results.

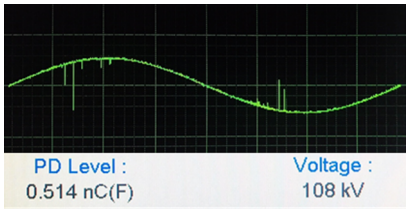

Fig. 14. Partial discharges at 108 kV_{rms} measured by conventional method.

Table 2
Voltages for testing HV cable with HFCT and filter A.

Waveform	Test	T_f/T_h [μs]	Values [kV]	
			V_{ACpeak}	V_{peak}
Impulse	1	3/56	–	274
	2	3/2000	–	274
Superimposed voltage	3	3/91	124	196

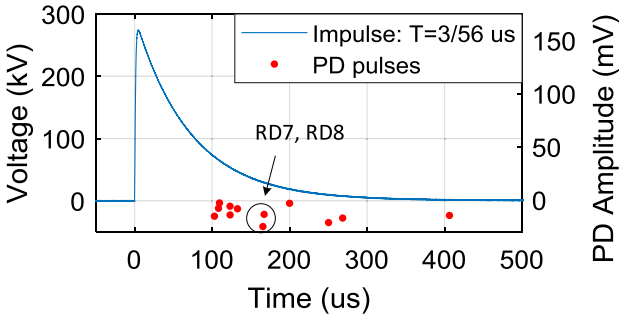

Fig. 15. PD occurrence measured under impulse voltage in test 1.

4.1. Partial discharges under impulse

The partial discharges from the cable joint were tested under impulse voltages as shown in Fig. 4a. A short impulse voltage with $T_f = 3$ μs and $T_h = 56$ μs was firstly applied on the cable in test 1. Fig. 15 shows the observed PDs with their polarities and amplitudes under this impulse. The PDs shown in Fig. 15 were measured by HFCT 1, with which the polarity of measured PD is the same as the polarity of applied voltage (see Section 3.3). All PDs were detected on the wave tail with negative polarities, which are referred to as reverse discharges (RD) according to Densley [30] (see Section 5). The pulse shapes of the reverse discharges RD7 and RD8 measured by the two HFCTs are given in Fig. 16a. The pulse measured by HFCT 1for RD7 and RD8 are both negative. The opposite polarities for each PD event as observed by HFCT 2 shows that the discharges originate from the cable joint internally.

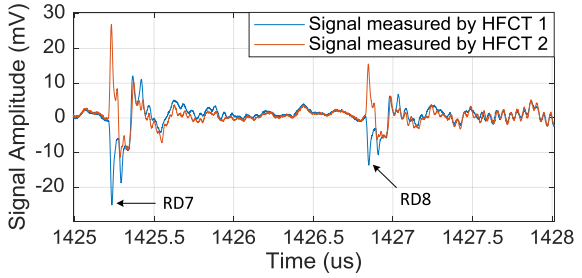

(a). Pulses of partial discharges RD7 and RD8 under impulse voltage.

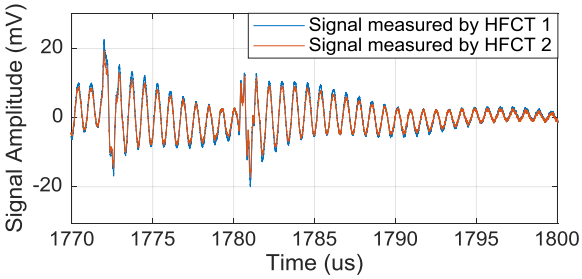

(b). Pulses of measured disturbance under impulse voltage.

Fig. 16. TRPD pulses of signals measured under impulse voltage in test 1.

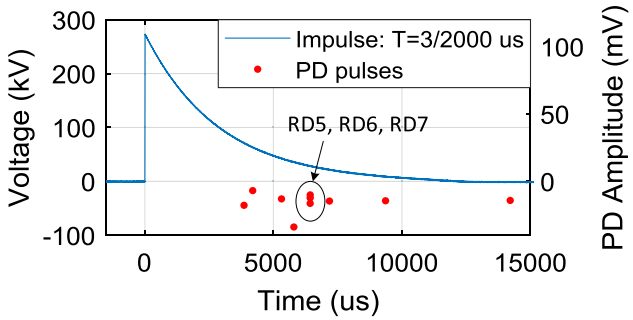

Fig. 17. PD occurrence measured under impulse voltage in test 2.

The impulse application generated a lot of disturbance which was also captured by the HFCTs. Fig. 16b shows typical disturbances. The two signals from the two HFCTs are always in phase, which indicates that the disturbance is external to the cable joint. Such polarity recognition contributes to separate PD from disturbance in the analysis stage.

A longer impulse voltage with $T_f = 3\,\mu s$ and $T_h = 2000\,\mu s$ was next applied to the cable in test 2. The observed PDs are shown in Fig. 17. Similar to test 1, PDs were only detected on the wave tail with negative polarities. Fig. 18 shows the pulse shapes of the three reverse discharges RD5, RD6 and RD7, which occurred in series.

Test 1 and test 2 show that, the PD measuring system is able to measure signals, including PD and disturbance, under impulse voltages. Moreover, using the pulse shape and pulse polarity, it is possible to identify PD from the cable joint and separate PD from disturbance.

4.2. Partial discharges under superimposed AC and impulse voltages

The HV cable system was then subjected to the superimposed voltages. In test 3, the superimposed voltage waveform, as shown in Fig. 4b, was applied to the cable system. The AC voltage was set at 124 kV_{ACpk}, which is the nominal operating voltage of the cable system. Since this AC voltage is below the PDIV of 147 kV_{ACpk}, no PD would occur. The applied impulse voltage with $T_f = 3\,\mu s$ and $T_h = 91\,\mu s$ made the superimposed voltage reach to a peak value of 196 kV_{pk}, which is well above the PDIV. During the test, the AC voltage was continuously applied before the impulse, under which no PD occurred. Then the impulse was superimposed on the AC voltage. After the impulse, the AC voltage was continuously applied until no more PDs were observed. The measurement results are shown in Figs. 19 and 20.

Fig. 19a shows the observed PD activity over time under the superimposed voltage. Before the impulse, no PD occurred under the AC voltage as expected. When the impulse was applied on the cable, PD initiated, and then reoccurred for around 360 s under AC voltage. Fig. 19b shows the PD occurrence during the first eight cycles after the impulse. During the impulse moment, no PD could be observed. From the first negative cycle after the impulse, PD started to occur. With time,

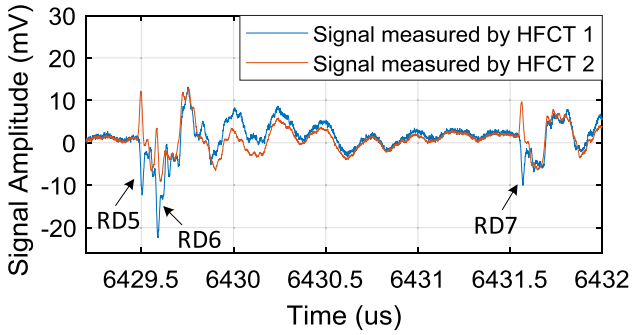

Fig. 18. TRPD pulses of RDs measured under impulse voltage in test 2.

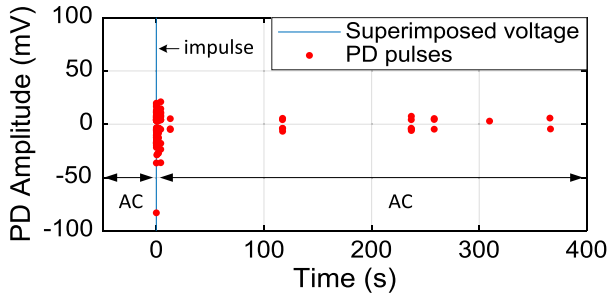

(a). PD occurrence under superimposed voltage over time.

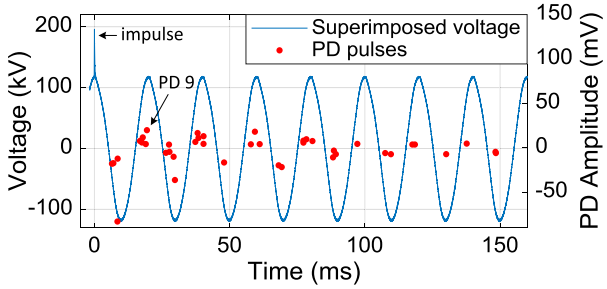

(b). PD occurrence during the first eight cycles after the impulse.

Fig. 19. PD occurrence measured under superimposed voltage in test 3.

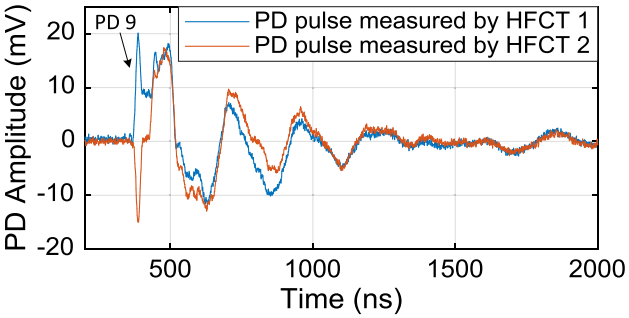

Fig. 20. TRPD pulses of PD9 measured under superimposed voltage in test 3.

the number of PD decreased. The pulse shape of one PD from the positive cycle is given as PD9 in Fig. 20.

Test 3 shows that, the PD measuring system is able to measure signals under superimposed voltages. However, so far no PD could be detected during the impulse moment.

5. Improved PD measurements

The previous tests have proven that, the deployed PD measuring system is capable to measure PD from the cable joint under impulse and superimposed voltages.

According to Densley [30], PD initiates at the impulse both during the front time and the tail time. PD occurring during the front time near the peak of the impulse is referred to as main discharge with positive polarity. PD occurring during the tail time is referred as reverse discharge with negative polarity. However, in the previous tests under impulse voltages, only reverse discharges (RD) were detected during the tail time. No main discharges (MD) have been observed during the front time. For superimposed voltages, PDs were observed when the impulse was finished but not during the impulse moment. The reason is, the disturbance generated by the impulse application obstructed the observation of PDs during the front time of impulses. As shown in Fig. 5, besides PD signals, a large signal was also induced in the HFCT during the impulse application, which was regarded as disturbance during the PD measurement. As a result, the signal captured by the HFCT was a superposition of the induced disturbance and the PD

signals. For safety purpose, the captured signal firstly went through filter A and is then clipped by the TVS (Section 2.3). For measurement purpose, the vertical scale on the oscilloscope was set to 20–30 mV/division (Section 3.3) and the signal was then clipped as well by the vertical observation window. In the end, the signal on the oscilloscope displayed a large disturbance being clipped lasting for a certain period. After that period, the disturbance was gone and the PD signals could be observed clearly. However, if PDs occurred during this disturbance period, they might be undetectable. In case PDs occurred at the moment where the disturbance was larger than the 12 V threshold of the TVS, the PD signals would be clipped. If PDs occurred when the disturbance was smaller than 12 V but larger than the vertical observation window, they would still be clipped. It is possible to increase the vertical observation window. But in this case, the signal (in millivolt) to noise (in volt) level is too small so that it is impossible to decouple the PD signals from the disturbance signals. Only if PDs occurred when the disturbance was within the observation window, there was a chance to observe them.

There are several options to cope with this issue. The signals can be measured with a higher threshold of TVS, and a larger vertical scale of the oscilloscope. However, in this way, the signal to noise issue still exists. Another option is to use a coaxial attenuator to attenuate the captured signals. However, both the PD signals and the disturbance signals will be attenuated. Thus, for measuring PD, using an attenuator is considered not suitable.

In this work, to solve the problem, another filter/suppressor unit was used, which consists of a band-pass filter with a bandwidth of 1.38–90.2 MHz, a TVS and a spark gap. Same as filter A, all the elements are integrated in a box, named filter B. During measurement, filter B was added before filter A. Fig. 21 gives the characteristics of the new measuring configuration combined with the HFCT, the connecting coaxial cable, the filter A and the filter B. To evaluate the effectiveness of adding filter B, the signal was measured again under the impulse voltage as in Secttion 2.3 and test 2. Fig. 22 shows the measured signal in time and frequency domains. From the point of view of observing PD on the oscilloscope in time domain, it can be seen from Fig. 22a that, the large disturbance lasts for 100–150 µs without filter B. During this period, it is difficult to observe or decouple the PD signals from the disturbance. This period is named as dead zone. After adding filter B, the disturbance has been suppressed and the dead zone has been reduced to around 40 µs. In this case, any PD occurring after 40 µs is supposed to be detectable.

The disturbance was also measured under impulse voltages in test 1 and 3 with different voltage values. With higher voltage and longer time of the impulse, the disturbance tended to have larger amplitude and longer dead zone. In all cases, filter B helped to suppress the disturbance and to decrease the dead zone.

The performance of the PD measuring system has been improved by adding filter B. However, the resulting dead zone is still longer than the impulse front time of 3 µs, as shown in Fig. 23. In order to detect the main discharges during the front time, impulses with longer front time of 300 µs were applied to the cable system. In this case, main discharges were expected to be detectable during the front time. The tests performed with filter A + B are listed in Table 3 The results are explained in the following chapters.

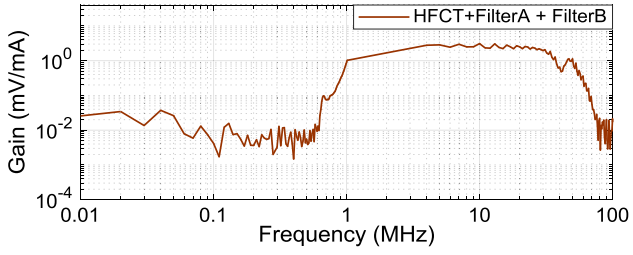

Fig. 21. Characteristics of new measuring configuration.

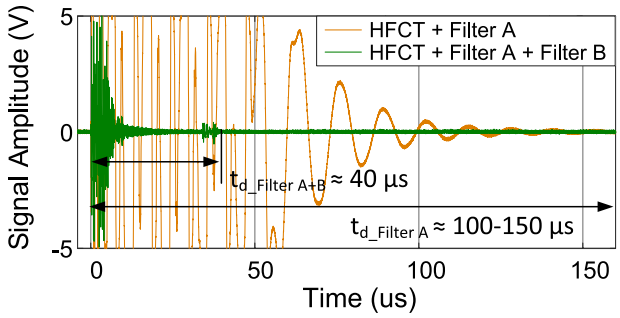

(a). Measured disturbance in time domain shown on oscilloscope.

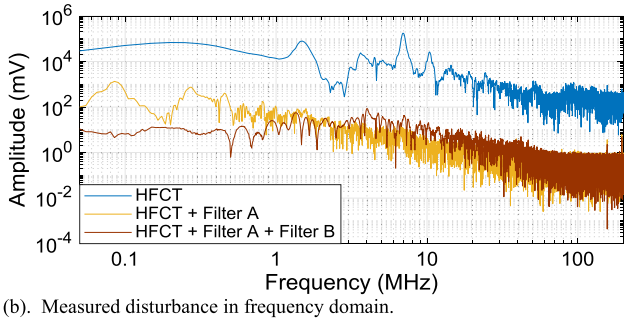

(b). Measured disturbance in frequency domain.

Fig. 22. Disturbance during impulse (T_f/T_h = 3/2000 µs) application measured with different configurations.

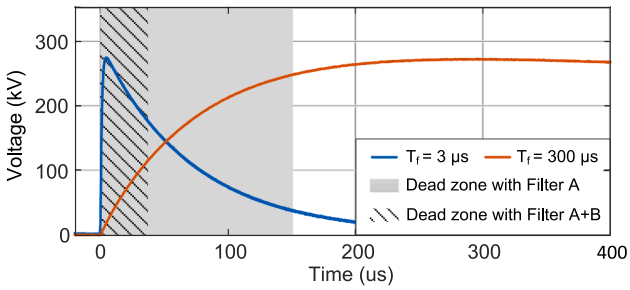

Fig. 23. Signals measured with only filter A and filter A + B.

Table 3
Voltages for testing HV cable with HFCT, filter A + B.

Waveform	Test	T_f/T_h [µs]	Values [kV]	
			V_{ACpk}	V_{pk}
Impulse	4	300/2650	–	274
Superimposed voltage	5	93/714	124	196
	6	93/845	124	194

5.1. Partial discharges under AC

The HV cable system was tested again under an AC voltage of 108 kV_{rms}. PRPD patterns and TRPD pulses of partial discharges from the cable joint were measured with the new PD measuring configuration. Fig. 24 shows the PRPD patterns. Fig. 25a shows the pulse shapes of one PD event. The opposite polarity appears at the first peak and the reversed at the second peak. Afterwards the two pulses oscillate in phase. Based on this feature, given the case as shown in Fig. 25b, PD 2 was recognized as another PD event right after PD 1 instead of the residual oscillation of PD 1. The shape distortion produced by the new filter B doesn't jeopardize the pulse polarity recognition.

Moreover, adding filter B also leads to a decrease in the measured PD amplitude. Fig. 26 shows the pulses of one PD event simultaneously

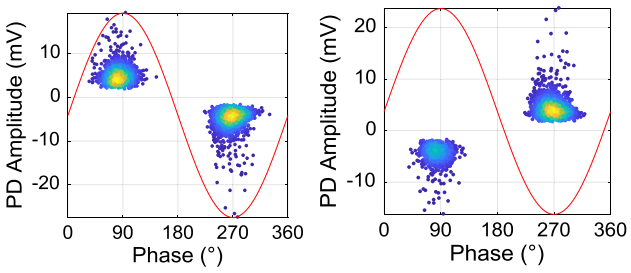

(a). HFCT 1 (b). HFCT 2

Fig. 24. PRPD patterns of partial discharges from cable joint measured with filter A + filter B.

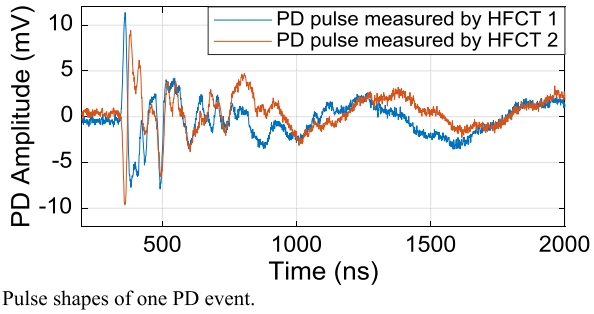

(a). Pulse shapes of one PD event.

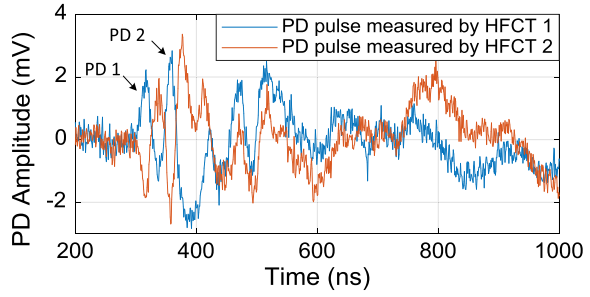

(b). Pulse shapes of two PD events in series.

Fig. 25. TRPD patterns of partial discharges from cable joint measured with filter A + B.

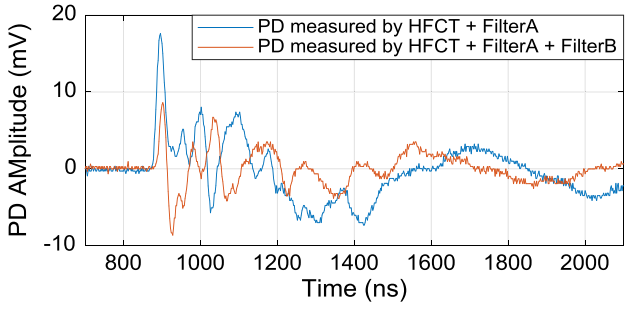

Fig. 26. Pulse shapes of one PD event measured with filter A and filter A + B.

measured with and without filter B under 108 kV_{rms} AC. By using filter B, the amplitude of measured PD signal has been decreased around 50%. In case the decreased signal is close to the trigger level, it is very likely that this PD signal will not trigger the acquisition. As a result, using filter B may influence the detection of small PDs.

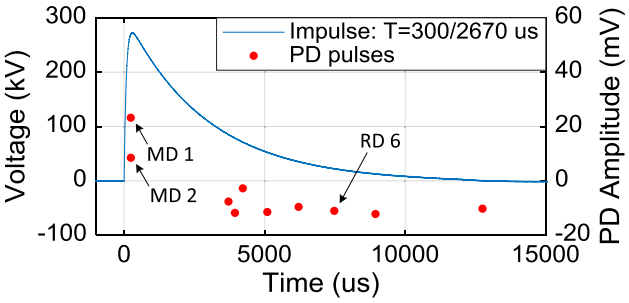

Fig. 27. PD occurrence measured under impulse voltage in test 4.

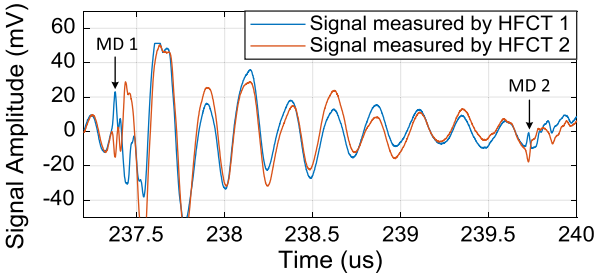

(a). TRPD pulses of MD1 and MD2 measured under impulse voltage.

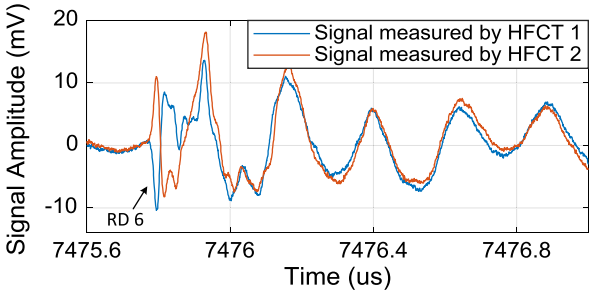

(b). TRPD pulses of RD6 measured under impulse voltage.

Fig. 28. TRPD pulses of PDs measured under impulse voltage in test 4.

5.2. Partial discharges under impulse

The cable system was next subjected to a switching-like impulse with T_f = 300 μs and T_h = 2650 μs in test 4. The observed PDs are shown in Fig. 27. In this test, main discharges with positive polarities were detected during the front time near the impulse peak at 237.4 μs and 239.7 μs, indicated as MD1 and MD2. During the impulse tail time, more reverse discharges occurred. Fig. 28a shows the pulse shapes of the two main discharges MD1 and MD2. Fig. 28b shows one reverse discharge RD6.

5.3. Partial discharges under superimposed AC and impulse

In test 3, PD was measured with filter A under a superimposed voltage with T_f = 3 μs. In test 5 and 6, the same voltage values as in test 3 but with longer impulse front time of T_f = 93 μs were applied to the cable system. Figs. 29 and 30 show the measurement results with only filter A in test 5. Similar to test 3, PDs were initiated by the impulse starting from the first negative cycle, and lasted for around 22 s under AC voltage. No PD were detected during the impulse moment. In test 6, the same superimposed voltage was applied and PD were measured

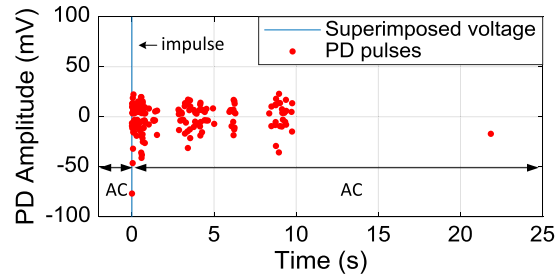

(a). PD occurrence over time.

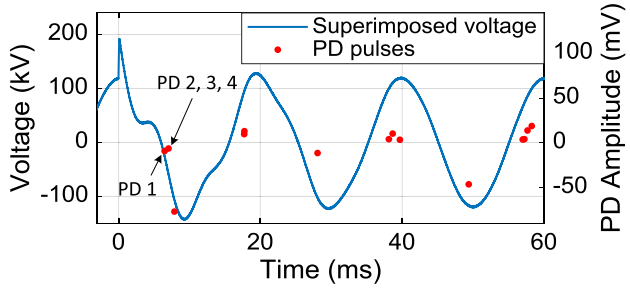

(b). PD occurrence during the first three cycles.

Fig. 29. PD occurrence measured under superimposed voltage in test 5.

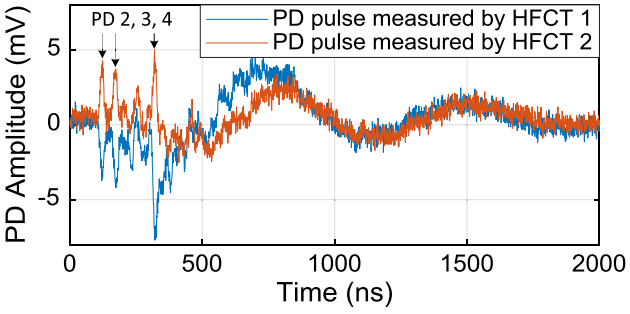

Fig. 30. TRPD pulses of PD2, PD3 and PD4 measured under superimposed voltage in test 5.

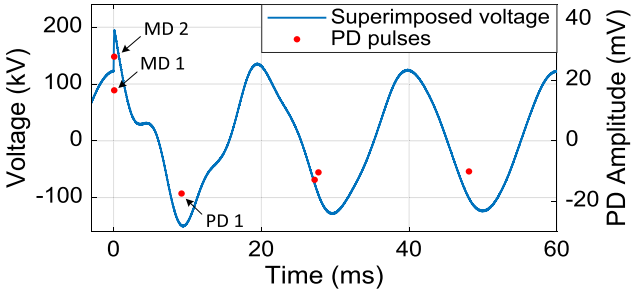

Fig. 31. PD occurrence measured under superimposed voltage in test 6.

adding filter B. The measurement results are shown in Figs. 31 and 32. With filter B, main discharges were detected during the front time near the impulse peak at 91.6 μs, shown as MD1 and MD2 in Fig. 31. The pulses shapes of MD1, MD2 near the impulse peak and PD1 under AC are given in Fig. 32.

By adding the filter B, the PD measuring system is able to measure both main discharges during the front time as well as the reverse discharges during the tail time, as long as the impulse voltage has a front

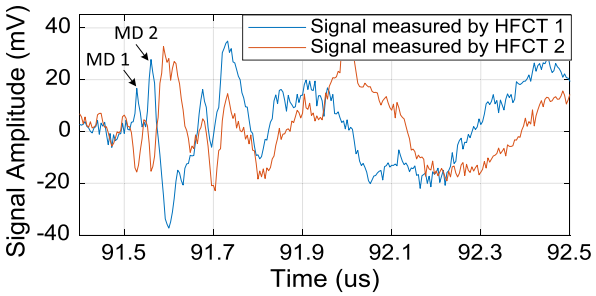

(a). TRPD pulses of MD1 and MD2 measured under impulse voltage.

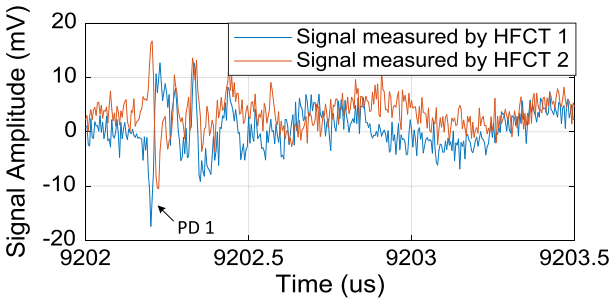

(b). TRPD pulses of PD1 measured under impulse voltage.

Fig. 32. TRPD pulses of PDs measured under superimposed voltage in test 6.

time longer than the dead zone of the PD measuring system. On the other hand, small PD signals might be missing during the acquisition, due to attenuation produced by filter B and the trigger level. As a conclusion, whether to use filter B or not depends on the purpose of the test. If it is aimed to detect PDs during the entire impulse or superimposed transient moment, using filter B will help to decrease the dead zone. If it is more important to observe all the PD activities, removing filter B will increase the chance of the detection of small PD events.

6. Conclusions

In this work, an unconventional PD measuring system was investigated to find a way to identify and measure PD in a HV cable system under laboratory conditions during impulse and superimposed AC voltage conditions. Two HFCTs were installed at the two ends of the cable joint with the same polarity. The signals captured by the HFCTs went through band-pass filters after which both were acquired by a digital oscilloscope. The PD data were then analyzed by the software PDflex and presented in PRPD pattern and TRPD pulses.

The measurements under impulse and superimposed voltages show that, the deployed PD measuring system is able to identify and measure PD in the joint during the impulse conditions without and with AC superposition. Under these conditions the safety of equipment and human is ensured. The performance is achieved by using filters and transient voltage suppressors, and by post processing data techniques in PDflex.

The installed HFCTs measure the signals internally to the cable joint with opposite polarities while externally to the joint with equal polarities. Such polarity recognition allows to identify PD from the cable joint, and discern PD from disturbances. The disturbance separation obtained by the polarity recognition and filters A and B is considered useful especially during the impulse test, since many disturbances enter the measuring system during the impulse application.

The applied band-pass filters, spark gaps and transient voltage

suppressors contribute to disturbance suppression and safety, which is a challenge in PD measurements under impulse. Filter A, equipped with a TVS and a spark gap, helps to protect the oscilloscope. By adding filter B, the extra band-pass filter helps to further suppress the disturbance and reduce the detection dead zone without detriment to the polarity recognition and having a good balance between pulse shape distortion and pulse attenuation. As a result, PD can be detected during the impulse front time.

As an outcome, PD occurrence are presented with their pulse shapes and amplitudes during impulse and superimposed voltages as well as under AC voltage before and after impulses.

The presented PD measuring system is instrumental for investigating the effect of transients on HV cable system in laboratory conditions. The effect of transients on HV cable system and the usefulness of the knowledge regarding such effect for on-site testing are to be investigated in future work.

Declaration of Competing Interest

The authors declared that there is no conflict of interest.

Acknowledgement

Authors would like to thank TenneT B.V. of the Netherlands for funding this project and providing technical advices and support.

Table 4
Setting of Marx impulse generator for generating different test impulses.

Waveform	C_{load} [nF]	Test	Impulse characteristics			Value/setting of each stage	
			T_f [μs]	T_h [μs]	C [nF]	R_f [Ω]	R_h [Ω]
Impulse	4.25	1	3	56	500	Stage 1–5: 35	Stage 1–5: 137
		2	3	2000		Stage 1–5: 35	Stage 1–5: 6000
		4	300	2650		Stage 1–5: 3400	Stage 1–5: 6000
Superimposed voltage	2.25	3	3	91		Stage 1–5: 35	Stage 1–5: 137
		5	93	714		Stage 1: 500, Stage 2–5: 35	Stage 1: 1325, Stage 2–5: 2170
		6	93	845		Stage 1: 500, Stage 2–5: 35	Stage 1–3: 137, Stage 4–5: 6000

Appendix

The setting of the impulse generator for generating different impulse waveforms are given in Table 4.

References

[1] Gulski E, Smit JJ, Wester FJ. PD knowledge rules for insulation condition assessment of distribution power cables. IEEE Trans Dielectr Electr Insul 2005;12(2):223–39.
[2] Stone GC. Partial discharge diagnostics and electrical equipment insulation condition assessment. IEEE Trans Dielectr Electr Insul 2005;12(5):891–904.
[3] CIGRÉ WG B1.28. On-site partial discharge assessment on HV and EHV cable systems. Technical Brochure 728; May 2018.
[4] CIGRÉ WG D1.33. High-voltage on-site testing with partial discharge measurement. Technical Brochure 502; June 2012.
[5] IEC 60270:2000. High-voltage test techniques-partial discharge measurements; March, 2001.
[6] Lindell E, Bengtsson T, Blennow J, Gubanski SM. Measurement of partial discharges at rapidly changing voltages. IEEE Trans Dielectr Electr Insul 2008;15(3):823–31.
[7] Rodrigo Mor A, Castro Heredia LC, Harmsen DA, Muñoz FA. A new design of a test platform for testing multiple partial discharge sources. Int J Electr Power Energy Syst 2018;94:374–84.
[8] CIGRÉ WG D1.33. Guidelines for unconventional partial discharge measurement. Technical Brochure 444; December 2010.
[9] IEC/TS 62478 - Ed 1.0. High voltage test techniques—measurement of partial discharges by electromagnetic and acoustic methods; August 2016.
[10] Rodrigo A, Llovera P, Fuster V, Quijano A. High performance broadband capacitive coupler for partial discharge cable tests. IEEE Trans Dielectr Electr Insul 2013;20(2):479–87.
[11] IEC/TS 61934 - Ed 2.0. Electrical insulating materials and systems-electrical measurement of partial discharges (PD) under short rise time and repetitive voltage impulses; 2011.
[12] Hayakawa N, Yoshitake Y, Koshino N, Ueda T, Okubo H. Impulse partial discharge characteristics and their mechanisms under non-uniform electric field in N/sub 2// SF/sub 6/ gas mixtures. IEEE Trans Dielectr Electr Insul 2005;12(5):1035–42.
[13] Ji H, Ma G, Li C, Pang Z, Zheng S. Influence of voltage waveforms on partial discharge characteristics of protrusion defect in GIS. IEEE Trans Dielectr Electr Insul 2016;23(2):1058–67.
[14] Deng J, et al. Partial discharge characteristics of uniform gap in oil-impregnated paper insulation under switching impulse voltage. IEEE Trans Dielectr Electr Insul 2016;23(6):3584–92.
[15] Zhang L, Han X, Li J. Partial discharge detection and analysis of needle-plane defect in SF6 under negative oscillating lightning impulse voltage based on UHF method. IEEE Trans Dielectr Electr Insul 2017;24(1):296–303.
[16] Ren M, Dong M, Ye R, Liu Y. Partial discharge test under standard oscillating impulses on a gas-insulated bus with artificial metal particle defects on the insulator surface. IEEE Trans Dielectr Electr Insul 2016;23(6):3593–601.
[17] Garcia-Colon VR, Estrada García JA, Ley Cotoc WK, Betancourt Ramirez E. Development of ultra wide band partial discharge sensors for power transformer winding insulation. Cigre Session; 2008, paper D1-211.
[18] Illias HA, Tunio MA, Mokhlis H, Chen G, Bakar AHA. Experiment and modeling of void discharges within dielectric insulation material under impulse voltage. IEEE Trans Dielectr Electr Insul 2015;22(4):2252–60.
[19] Hayakawa N, Yamaguchi R, Ukai Y, Kojima H, Endo F, Okubo H. Partial discharge activities under AC/impulse superimposed voltage in LN2/polypropylene laminated paper insulation system for HTS cables. J Phys Conf Ser 2010;234(3):032020.
[20] Nikjoo R, Taylor N, Edin H. Effect of superimposed impulses on AC partial discharge characteristics of oil-impregnated paper. IEEE Trans Dielectr Electr Insul 2016;23(6):3602–11.
[21] Blackburn TR, Phung BT, Hao Z. On-line partial discharge monitoring for assessment of power cable insulation. In: Proceedings of 2005 international symposium on electrical insulating materials, 2005. (ISEIM 2005), vol. 3; 2005. p. 865–8.
[22] Nattrass DA. Partial discharge measurement and interpretation. IEEE Electr Insul Mag 1988;4(3):10–23.
[23] Ahmed NH, Srinivas NN. On-line partial discharge detection in cables. IEEE Trans Dielectr Electr Insul 1998;5(2):181–8.
[24] Kreuger FH. Industrial High Voltage Vol. II. Delft, The Netherlands: Delft University Press; 1992.
[25] On-line Partial Discharge Products and Test Services | HVPD. [Online]. Available: https://www.hvpd.co.uk/. [Accessed: 08-Mar-2019].
[26] Hu X, Siew WH, Judd MD, Peng X. Transfer function characterization for HFCTs used in partial discharge detection. IEEE Trans Dielectr Electr Insul 2017;24(2):1088–96.
[27] Partial discharges software - PDflex: PD parameters and clustering. PDFlex - Unconventional partial discharge analysis. [Online]. Available: http://pdflex.

tudelft.nl/. [Accessed: 28-Aug-2018].
[28] Mor AR, Heredia LCC, Munoz FA. Estimation of charge, energy and polarity of noisy partial discharge pulses. IEEE Trans Dielectr Electr Insul 2017;24(4):2511–21.
[29] Mor AR, Morshuis PHF, Smit JJ. Comparison of charge estimation methods in partial discharge cable measurements. IEEE Trans Dielectr Electr Insul 2015;22(2):657–64.
[30] Densley RJ, Salvage B. Partial discharges in gaseous cavities in solid dielectrics under impulse voltage conditions. IEEE Trans Electr Insul 1971;EI-6(2):54–62.

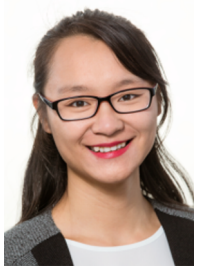

Jiayang Wu was born in Nanjing, China in 1988. She received the BSc degree in electrical engineering from the Southeast University, Nanjing, China, in 2010, and the MSc degree in electrical power engineering from the RWTH Aachen University of Technology, Aachen, Germany in 2013. She is currently a Ph.D candidate in the Electrical Sustainable Energy Department at Delft University of Technology, Delft, The Netherlands. Her current research focuses on the effects of transients on the high voltage cable systems.

Armando Rodrigo Mor is an Industrial Engineer from Universitat Politècnica de València, in Valencia, Spain, with a Ph.D. degree from this university in electrical engineering. During many years he has been working at the High Voltage Laboratory and Plasma Arc Laboratory of the Instituto de Tecnología Eléctrica in Valencia, Spain. Since 2013 he is an Assistant Professor in the Electrical Sustainable Energy Department at Delft University of Technology, Delft, The Netherlands. His research interests include monitoring and diagnostic, sensors for high voltage applications, high voltage engineering, and HVDC.

Paul van Nes (Amsterdam 1957). Took a degree in both electrical engineering and in mechanical engineering. He joint KEMA in 1982, he was first a mechanical test engineering, occupied with the commissioning testing of power station. Later he moved to the High Voltage Laboratory of KEMA were he was test engineer in the field type testing of High Voltage equipment for companies from all over the globe. In 1998 he was invited to become head of the high voltage laboratory of Delft University of Technology. Nowadays, he guides master students and PhD students in their laboratory research.

Johan J. Smit is professor at the Delft University of Technology (The Netherlands) in High Voltage Technology and Management since 1996 and emeritus since 2015. After his graduation in experimental physics he received his PhD degree from Leiden University in 1979. After his research in cryogenic electromagnetism at the Kamerlingh Onnes Laboratory, he was employed as T&D research manager at KEMA's laboratories in Arnhem-NL for 20 years. Furthermore he was director of education in electrical engineering, supervisory board member of the power transmission company of South Holland, and CEO of the asset management foundation Ksandr for 10 years. In 2003 he was general chairman of the International Symposium on HV Engineering in Delft. He is TC-honorary member of CIGRE and past chairman of CIGRE D1 on Materials & Emerging Technologies. Currently he is convener of the area Substation Management for CIGRE B3 and he holds the international chair of Technical Committee IEC112 on Electrical Insulation Systems.